

## CXCR4 and matrix metalloproteinase-2 are involved in mesenchymal stromal cell homing and engraftment to tumors

CHAO SONG<sup>1,2,3</sup> & GANG LI<sup>1,2,4,5</sup>

<sup>1</sup>Stem Cell and Regeneration Program, Li Ka Shing Institute of Health Sciences, The Chinese University of Hong Kong, Prince of Wales Hospital, Shatin, Hong Kong, SAR, PR China, <sup>2</sup>Department of Orthopaedics and Traumatology, The Chinese University of Hong Kong, Prince of Wales Hospital, Shatin, Hong Kong, SAR, PR China, <sup>3</sup>Urology Department, Renmin Hospital of Wuhan University, Wuhan, Hubei Province, PR China, <sup>4</sup>The Hong Kong Jockey Club Sports Medicine and Health Sciences Centre, The Chinese University of Hong Kong, Hong Kong, SAR, PR China, and <sup>5</sup>MOE Key Laboratory of Regenerative Medicine, School of Biomedical Sciences, Basic Medical Sciences Building, The Chinese University of Hong Kong, Shatin, Hong Kong, SAR, PR China

### Abstract

**Background aims.** Bone marrow-derived mesenchymal stromal cells (BMSC) have been shown to migrate to injury, ischemia and tumor microenvironments. The mechanisms by which mesenchymal stromal cells (MSC) migrate across endothelium and home to the target tissues are not yet fully understood. **Methods.** We used rat BMSC to investigate the molecular mechanisms involved in their tropism to tumors *in vitro* and *in vivo*. **Results.** BMSC were shown to migrate toward four different tumor cells *in vitro*, and home to both subcutaneous and lung metastatic prostate tumor models *in vivo*. Gene expression profiles of MSC exposed to conditioned medium (CM) of various tumor cells were compared and revealed that matrix metalloproteinase-2 (MMP-2) expression in BMSC was downregulated after 24 h exposure to tumor CM. Chemokine (C–X–C motif) Receptor 4 (CXCR4) upregulation was also found in BMSC after 24 h exposure to tumor CM. Exposure to tumor cell CM enhanced migration of BMSC toward tumor cells. Stromal Cell-Derived Factor (SDF-1) inhibitor AMD3100 and MMP-2 inhibitor partly abolished the BMSC migration toward tumor cells *in vitro*. **Conclusions.** These results suggest that the CXCR4 and MMP-2 are involved in the multistep migration processes of BMSC tropism to tumors.

**Key Words:** cell migration, CXCR4, matrix metalloproteinase-2, mesenchymal stromal cells, tumors

### Introduction

Bone marrow-derived mesenchymal stromal cells (BMSC) have been shown to migrate to injury, ischemia and tumor microenvironments *in vivo* and *in vitro*. Intravenous delivery of BMSC results in their specific homing to sites of injury and improves recovery in animal models of skin injury (1), stroke and myocardial infarction (2). Mesenchymal stromal cells (MSC) have also been used for targeted delivery of therapeutic gene products to tumor microenvironments in animal models (3) and the therapeutic use of MSC is being explored for various disease conditions (4). Considered as wounds that never heal (5), tumor microenvironments share many similarities with

tissue repair processes, which can attract specific homing of MSC (6,7). Taking advantage of MSC homing properties, MSC may be isolated, expanded and modified *ex vivo* and used as delivery vehicles for anti-tumor agents. Understanding the factors that regulate MSC homing/migration and engraftment into target tissues such as tumors will help to improve the application of MSC as therapeutic anti-tumor vehicles (7).

Chemokines are key mediators of selective cell migration in neurodegenerative diseases and related inflammatory processes. Human MSC express CC, CXC and CX3C receptors, such as CCR1, CCR2, CCR7, CCR8, CXCR1, CXCR2, CXCR3, CXCR,

Author contributions: Chao Song, conception and design, collection and/or assembly of data, data analysis and interpretation, manuscript writing; Gang Li, conception and design, data analysis and interpretation, manuscript writing, administrative support, financial support, final approval of manuscript.

Correspondence: Professor **Gang Li**, Department of Orthopaedics and Traumatology, The Chinese University of Hong Kong, Prince of Wales Hospital, Shatin, Hong Kong, SAR, PR China. E-mail: gangli@ort.cuhk.edu.hk

(Received 10 October 2010; accepted 12 November 2010)

ISSN 1465-3249 print/ISSN 1477-2566 online © 2011 Informa Healthcare  
DOI: 10.3109/14653249.2010.542457

CXCR6 and CX3CR1, at both gene and protein levels (8–12). Many cytokines and their receptors are involved in regulating the migration of MSC, such as Toll-like receptors (13), hepatocyte growth factor (HGF) (14), insulin-like growth factor (IGF) types 1 and 2 (15–17), Vascular Endothelial growth factor (VEGF) (18), platelet-derived growth factor (PDGF) -BB and -AB, epidermal growth factor (EGF), heparin-binding-like growth factor (HB-EGF), transforming growth factor (TGF)-alpha, fibroblast growth factor (FGF)-2 and thrombin. PDGF-BB has shown the greatest effect on MSC migration in some studies, and various combinations of these factors have further enhanced the migration of MSC (19). As the tumor environments secrete some of these cytokines and chemokines, they may guide the migration of MSC to tumors (6,20). Expression and synthesis of matrix metalloproteinase in BMSC is also necessary for their mobilization and homing processes, which require invasion through extracellular matrix (ECM) barriers (21). Although some molecules have been identified in the MSC homing process, the mechanisms by which MSC migrate across endothelium and home to the target tissues are not yet fully understood.

The homing of MSC is a multistep process that depends on a timely and spatially orchestrated interplay between chemokines, cytokines and proteases. With this study, we aimed to test the migration mechanisms of BMSC toward tumor cells *in vitro* and examine the distribution of systemically delivered BMSC in tumor-bearing animals.

## Methods

### Isolation and culture of BMSC

Green fluorescent protein (GFP)-transgenic rats (SLC Inc., Shizuoka, Japan) or normal Sprague–Dauley rats were raised and killed under an animal license issued by the Hong Kong SAR Government and local ethical committee. Bone marrow was harvested from the long bones and layered onto Lymphoprep™ (1.077 g/mL; Nycomed, Birmingham, UK) for centrifugation at 850 *g*, 25 min. The isolated mononuclear cells, suspended in Dulbecco's modified Eagle medium (DMEM) containing 10% fetal bovine serum (FBS), 100 U/mL penicillin, 100 mg/mL streptomycin, 2.5 µg/mL fungizone and 2 mM L-glutamine (Invitrogen, Paisley, UK), were seeded into T75 flasks (Iwaki, Chiba, Japan) at a density of  $1 \times 10^5$  cells/cm<sup>2</sup> and incubated at 37°C in a humidified atmosphere with 5% CO<sub>2</sub>/95% air. Expanded cultures of BMSC were analyzed for chondrogenic, osteogenic and adipogenic differentiation *in vitro* to determine multipotency according to standard conditions as described previously (22).

### Tumor cell lines

The human tumor cell lines used for this study were breast cancer (MCF-7) and prostate cancer (PC3 and DU145); all were obtained from the American Tissue Culture Collection (ATCC, LGC, Standards, Middlesex, UK). The murine tumor cell line, RIF-1, was obtained from Cancer Research UK: London, England, UK. All cells were cultured in RPMI-1640 medium (Gibco Life Sciences, Grand Island, NY, USA) supplemented with 10% FBS, 100 U/mL penicillin, 100 mg/mL streptomycin and 2.5 µg/mL fungizone at 37°C in 5% CO<sub>2</sub>/95% air.

### Vector design and plasmid constructs

For construction of the Lentivirus (Lenti)-Luciferase (Luc)-Topo plasmid, a luciferase cassette was cloned by polymerase chain reaction (PCR) methods from the plasmid containing luciferase (a kind gift from Yao-Cheng Li, PhD, The Salk Institute for Biological Studies Gene Expression Laboratory, La Jolla, CA, USA). The primers used were: sense primer ACCA TGGAAGACGCCAAAACA and antisense primer TTAGCTTGTACAGCTCGTCCA. The PCR product of 2395 bp was purified and ligated directly with the Lenti-Topo plasmids (Invitrogen). The constructed plasmids were identified by restriction enzyme digestion and confirmed by sequencing analysis.

### Lenti-virus production and gene transduction

Vector particles were produced in 293T cells by transient co-transfection involving a four-plasmid expression system. Briefly, 293T cells were plated into 10-cm<sup>2</sup> plates ( $2 \times 10^6$  cells/well) and 24 h later transfer vector plasmid (such as Lenti-Luc-GFP) DNA (8 µg), helper plasmid plp-1 DNA (5.28 µg), helper plasmid plp-2 DNA (4 µg) and envelope plasmid plp-VSVG DNA (2.8 µg) added. Transfection by calcium phosphate in the presence of 25 µM chloroquine was carried out for 12–15 h. The medium was replaced and virus particles released into the medium were harvested 48–72 h after transfection. Virus particles were concentrated by centrifugation at 25 000 r.p.m. (30 000 *g*) at 4°C for 2 h using a Beckman SW28 rotor. Virus was titered by limited dilution of 293T cells according to protocols provided by Invitrogen. The gene transductions were carried out at the appropriate Multiplicity of infection (MOI) (10 for 293T or tumor cells, 50 for BMSC) in the presence of 8 µg/mL Polybrene. The transduced tumor cells and BMSC were selected further with 10 µg/mL Blasticidin. The stable transduction of the cells was confirmed by luciferase assay for luciferase expression.

### *Two-color flow cytometry analysis of luciferase-transduced BMSC*

All antibodies used were purchased from Dako Cytomation Ltd (Cambridge, UK), unless otherwise specified. Luciferase–GFP-transduced BMSC were used for flow cytometric analysis. The cells were washed in cold phosphate-buffered saline (PBS) buffer containing 5% bovine serum albumin (BSA; Sigma, Poole, UK). Separate aliquots of  $1 \times 10^5$  luciferase-labeled BMSC, which were collected after 2 weeks of Blasticidin selection, in a final volume of 50  $\mu$ L were used for incubation with antibodies for 30 min at 4°C in the dark. The antibodies used were 10  $\mu$ L polyclonal goat anti-rat CD31, CD44, CD45 and CD90, followed by 2  $\mu$ L secondary phycoerythrin (PE)-conjugated rabbit anti-goat antibodies, and cells without treatment of primary antibodies served as negative controls. The flow cytometry analysis was performed using a BD LSRFortessa™ cell analyzer with BD FACSDiva™ software.

### *Human prostate cancer xenograft animal model and systemic injection of luciferase BMSC*

To investigate the distribution of BMSC in tumor models, subcutaneous tumor implants were established by subcutaneous injection of  $2 \times 10^7$  PC3 or DU145 cells at three dorsal sites in nude mice (Nu/Nu nude mouse, 6 weeks old, male; Charles River, Wilmington, USA; three mice for PC3 and three mice for DU145). A lung tumor metastasis model was established in nude mice ( $n = 3$ ) by intravenous (i.v.) injection of  $5 \times 10^6$  PC3 cells in 200  $\mu$ L PBS through the tail vein. Rat–GFP–Luc–BMSC were injected as a suspension of  $10^6$  cells in 200  $\mu$ L PBS at day 7 after tumor cell administration. The number of tumor cells implanted or injected was decided based on pilot experimental data. For subcutaneous injection, at least  $1 \times 10^7$  tumor cells were used to ensure tumor growth within 2 weeks; as for the tumor cell systemic injection, the maximal number we could inject safely was  $5 \times 10^6$  cells, and care had to be taken regarding the injection speed, to make it as slow as possible to avoid sudden death of the animals caused by cells clotting in the blood vessels of the heart or other organs.

The distribution of Luc–BMSC was examined using an In Vivo Imaging System (IVIS 200; Xenogen, Alameda, CA, USA), following the manufacturer's instructions. In brief, D-luciferin (150 mg/kg) was administered through intraperitoneal injection 5 min before the imaging examination. The animals were anesthetized using 3% isoflurane (Abbott Laboratories, North Chicago, IL, USA) and placed on a warmed stage inside a camera box. The animals

received continuous exposure to 3% isoflurane to sustain sedation during imaging. Imaging times ranged from 10 s to 3 min, depending on the bioluminescence of the BMSC. The light emitted from the bioluminescent tumor cells was digitized and displayed electronically as a pseudo-color overlay on the gray-scale animal image. Regions of interest (ROI) from the displayed images were drawn around the tumor and quantified as photons/second (ph/s) using Living Image software provided with the IVIS 200 system. Background bioluminescence was in the range of  $3\text{--}6 \times 10^4$  ph/s. For the last time-point, after luciferin injection animals were killed and tissues of interest were excised, placed on black paper and imaged for 1 min. Tissues were subsequently fixed in 4% paraformaldehyde and prepared for paraffin embedding and standard histology and immunohistochemistry evaluations.

### *Actin polymerization assay*

PC3 cells were trypsinized and suspended in serum-free DMEM at a concentration of  $1 \times 10^7$ /mL. Low-melting point agarose (Invitrogen) was dissolved in serum-free DMEM at a final concentration of 2% w/w. The cell suspension was mixed with agarose medium at 37°C in a 2-mL syringe. The mixture (c. 1 mL) was then injected on to a plate with growth medium at room temperature (about 22°C), where a cell–agarose pellet was formed. The pellets were then transferred to the wells of six-well plates, in which the BMSC were plated in the adjacent areas and co-cultured at 37°C, 5% CO<sub>2</sub>, 95% air for 24 h. The co-culture was stopped by adding three volumes of 3.7% paraformaldehyde at room temperature for 10 min, followed by washing with PBS and permeabilization on ice for 2 min with 0.1% Triton–HEPES (20 mM HEPES, 300 mM sucrose, 50 mM NaCl, 3 mM MgCl<sub>2</sub>, 0.1% Triton X-100). Cells were then stained with fluorescein isothiocyanate (FITC)–phalloidin (2 mg/mL; Sigma) for 30 min at room temperature, washed and examined under a fluorescent microscope.

### *Cell migration and chemotaxis assays*

Conditioned media (CM) from tumor cells were harvested after 24 h culture, filtered and stored at –80°C for further use. Rat BMSC within passage 3 were detached and made into a single-cell suspension of  $10^6$  cells/mL. To assess cell migration,  $1 \times 10^5$  BMSC were dispersed onto the inserts of chemotaxis transwell dishes (Falcon 353097, 8.0- $\mu$ m pore size) and allowed to adhere for 1 h at 37°C. The transwell inserts were then transferred to the bottom chamber, which contained CM of the chosen

tumor cells. Normal culture medium only was used in the bottom chamber of a control group to measure the background migration of BMSC. For chemotaxis assay of CXCR4-luciferase-transduced BMSC,  $10^5$  cells were dispersed on to the transwell insert and Stromal Cell-Derived Factor (SDF)-1 $\alpha$  (100 ng/mL; PeproTech, Rocky Hill, US) added in the lower well, with normal BMSC serving as a control. AMD3100 (CXCR4-specific inhibitor; Sigma) and matrix metalloproteinase-2 (MMP-2) inhibitor (Calbiochem-Novabiochem Ltd, Nottingham, UK) were added into the transwell system to test the effect on BMSC migration. Each experiment was repeated three times. Cells were cultured in the transwell chambers for 12 h at 37°C in 5% CO<sub>2</sub>/95% air. Cells remaining attached to the upper surfaces of the filters were removed carefully with cotton swabs. Cells that had migrated to the lower surfaces of the filters were fixed with 95% alcohol, stained with Giemsa buffer and counted. Cells were randomly selected in five fields on each filter and the total number of cells from all fields was calculated and compared.

The chemotaxis assay was confirmed using the DUNN chemotaxis system for PC3 and DU145 tumor cells, as described previously (23). Briefly,  $10^6$  tumor cells were put into the outer ring of the chamber as the chemo-attractant, and the migration of BMSC was observed and recorded with a Nikon time-lapse microscope once every 10 min for an 11-h period. The cell migration was analyzed by AQM 2001 software (Kinetic Imaging Ltd, Manchester, UK) and Mathematic® 3.0 (Wolfram, Champaign, IL, USA).

#### Wound healing assay

A wound scrape migration assay was performed as described previously (24). Briefly, BMSC were plated in 3.5-cm culture dishes and grown to confluence, and a line wound in the middle of each well was made by scraping the cell layers with a 200- $\mu$ L plastic pipette tip. After washing with PBS, medium was changed to conditioned medium from tumor cells. For each experiment, the width of the cell-free area at six marked sites per well was measured in triplicate wells using inverse phase-contrast microscopy. Wound closure was quantified as the percentage of the starting distance between the wound edges after 12 and 24 h (analyzed by Image-Pro Plus 5.02; Media Cybernetics, Bethesda, MD, USA).

#### Reverse transcription-polymerase chain reaction examination

Reverse transcription (RT)-polymerase chain reaction reverse transcriptase (PCR) primers for genes of

interest were designed with the software Primer Premier 5 (Premier Biosoft International, Palo Alto, CA, USA). Preparation of RNA was carried out using Trizol (Invitrogen, Carlsbad, CA, USA) methods according to the manufacturer's instructions. RT were performed using a ImProm-II reverse transcription system (Promega, UK Ltd, Southampton, UK). The RT reaction mix was incubated at 25°C for 5 min for annealing and at 42°C for 1 h for RT. The RT was then thermally inactivated at 70°C for 15 min. The cDNA was amplified by a hot start enzyme, Promega PCR master mix, at 94°C for 2 min. The PCR cycles were 25 cycles of denaturation at 94°C for 30 s, annealing at 56°C for 45 s and extension at 72°C for 30 s, with finally 1 cycle at 72°C for 5 min and then holding at 4°C. The PCR products were run in 1% agarose gel (Invitrogen) and quantified using a gel scanner and software. The primers used in this study are listed in Table I.

#### Western blot

Western blot examination was carried out as described previously (25). Briefly, after co-culture with tumor cells in a six-well transwell insert (0.2  $\mu$ m; Nunc, Thermo Fisher Scientific, Kamstrup, Denmark), total cellular proteins were extracted with buffer containing 62.5 mM Tris-HCl (pH 6.8), 2% Sodium dodecyl sulfate (SDS), 1 mM Phenylmethanesulfonyl fluoride (PMSF) and Protease inhibitor cocktail (Roche, Indianapolis, IN, USA). Protein content was quantified with a bicinchoninic acid (BCA) protein assay kit (Pierce Technology, Perbio Science UK Ltd, Cramlington, UK) and equal amounts of protein were resolved by 10% SDS-PAGE. The protein was then transferred from the gel to PVDF membranes. Polyvinylidene fluoride PVDF membranes were incubated with primary antibodies, mouse monoclonal anti-rabbit antibodies of rabbit anti-human CXCR4 (Santa Cruz Biotechnology, Inc., Santa Cruz, CA, USA), rabbit anti-rat MMP-2 (Santa Cruz) and mouse anti  $\beta$ -actin (Sigma) overnight at 4°C, followed by PBS washes and immune detection with horseradish peroxidase-conjugated mouse anti-rabbit or rabbit anti-mouse immunoglobulins.

#### Statistics

Values were presented for each group as means  $\pm$  SD or expressed as a mean percentage of control  $\pm$  SD. The Student's *t*-test was used for comparison of mean values between different groups. Significance was considered when the *P*-value was less than 0.05.

## Results

#### MSC characterization

The multidifferentiation potentials of rat MSC were confirmed for their osteogenesis, chondrogenesis and

Table I. Primers used.

Name	Primers	Gene bank ID	Product size (bp)
MMP-2	Forward GCCTTTGCTCGGGCCTTA Reverse TGCTCCCATCGACCAAAGTT	NM_031054	107
MMP-9	Forward ACCCCATGTATCACTACCACGAG Reverse TCAGGTTTAGAGCCACGACCAT	NM_031055	91
MMP-14	Forward TCTTGGTGGCTGTGCATGA Reverse CTCGGTGTCCATCCACTGGTA	NM_031056	101
TIMP1	Forward CTTTGCAAACCTGGAGAGTGACA Reverse AGGCAAAGTGATCGCTCTGGT	NM_053819	91
TIMP2	Forward ACCCAGTCTCCCTCAGGTCTAAG Reverse CTTCATTCACGACGTCTGT	NM_031055	102
MMP-30	Forward TGACCCAGATCATGTTTGAGACC Reverse GTGGTACGACCAG AGGCATACA	NM_031144	91
CCR1	Forward CAGGTGACTGAAGTGATTGCCT Reverse AGCGGTATAGCCACATGCCT	NM_020542	122
CCR2	Forward CTGTGTGGTTGACATGCACTTAGA Reverse TTTGGCAATGTGCTTTCTGAA	NM_021866	84
CCR3	Forward GGCATCCAACGAAGAGGAACT Reverse GACGATGAACACCAGGGAATACA	NM_053958	151
CCR4	Forward GTTTGTGCTGTCTCTCCCGTT Reverse AGCCCACCAGGTACATCCAT	NM_133532	101
CCR5	Forward TCAACCCTGTCATCTATGCCTT Reverse GATCAGGATTGACTTGCTGGAA	NM_053960	126
CCR6	Forward TCACTTTCAATCCCCCTGTGA Reverse TTGGCCTCGGTGAAATTCAT	NM_001013145	151
CCR7	Forward ACCGTGGCCAATTTCAACA Reverse AGGTCGCTGCGGAACTTG	NM_199489	152
CCR9	Forward CCATTTCCACCAACATTGACAT Reverse TGGCTAATGCATCCCAGGTT	NM_172329	151
CX3CR1	Forward GTGGCCTTTGGGACCATCT Reverse CGTCAAGGCCAGGTTCA	NM_133534	151
CXCR3	Forward CCTGCCTCCGCTGTTTTTAGA Reverse CCTCTTCTCACACAGGGATGG	NM_053415	92
CXCR4	Forward TGGCTGACCTCCTCTTTGTCA Reverse AGGCTGATGAAGGCCAGGAT	NM_022205	151
PDGFRb	Forward TTGGCCTCTAAGAACTGTGTTTCAC Reverse CCAACTTGCCTCACAGATGA	AY090783	70
EGFR	Forward TGGACAACCCTCATGTATGC Reverse ACATAGTCCAGGAGGCAACC	M37394	100
HGFR	Forward GTCTTCAAGTAGCCAAGGGC Reverse AACATGCAGTTTCTTGACGC	NM-031517	82
GAPDH	Forward ATGACTCTACCCACGGCAAG Reverse CTGGAAGATGGTGATGGGTT	DQ403053	89

adipogenesis differentiation (Figure 1A–F). The phenotype of Lenti–luciferase-transduced GFP rat MSC did not change before and after gene transduction. The transduced MSC–GFP–Luc were positive for CD44 and CD90 and negative for CD45 and CD31, having similar phenotypes to the non-treated MSC (Figure 1G).

#### *Transwell, Dunn chamber chemotaxis assay, wound healing and action polymerization assays*

The membrane surface inside the bottom chamber facing the tumor cells was stained for the presence of migrated BMSC after 12 h co-culture. The numbers of BMSC migrating toward tumor cells (passing through the insert membranes) were significantly

higher compared with the control group ( $P < 0.05$ ). The BMSC migration potential was significantly enhanced when they were exposed to the tumor cell CM prior to the transwell assay in all tumor cells (Figure 2A). Neither of the two inhibitors totally inhibited BMSC migration toward the tumor cells. For the Dunn chemotaxis chamber assay, only randomly dispersed trajectories were recorded for the BMSC in the control group, where only medium was added to the outer ring of the chamber, suggesting the absence of a chemotactic response (Figure 2Ba). In contrast, BMSC showed directional migration toward DU145 and PC3 cell CM ( $P < 0.01$ ; Figure 1Bb,c). Twelve and 24 h after scratching, the distances between the wound edges were significantly reduced in all the tumor CM-treated

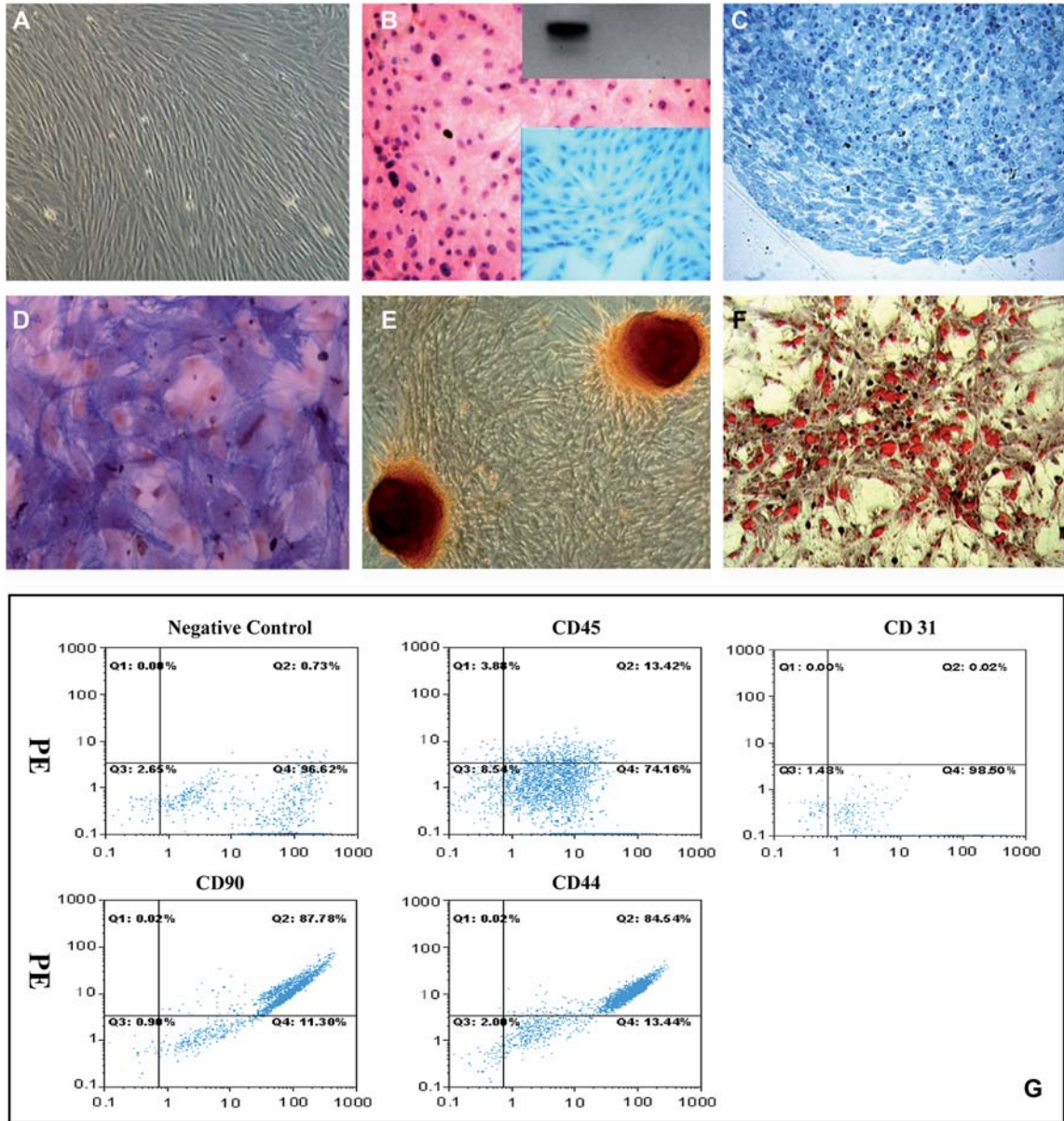


Figure 1. MSC differentiation assays and phenotype confirmation. (A) Rat BMSC reached confluence ( $\times 200$ ). (B) For chondrogenic induction, collagen type II was detectable by immunostaining in 2-dimensional (2-D) culture cells at day 22 ( $\times 200$ ; inset, negative control and Western blot of type II collagen). (C) After 4 weeks of chondrogenic induction culture, the cell pellets were sectioned and stained with Alcian Blue to show typical chondrocytes ( $\times 200$ ). (D) For osteogenic induction, the cells were positive for alkaline phosphatase (ALP) staining at day 14 ( $\times 400$ ). (E) The bone nodules were formed at day 28 as shown by Alizarine Red S stain ( $\times 200$ ). (F) For adipogenic induction, the accumulated lipid vacuoles were stained with Oil Red O at day 13 ( $\times 200$ ). (G) The phenotype of Lenti-luciferase-transduced GFP rat MSC did not change before and after gene transduction. The transduced MSC-GFP-Luc were positive for CD44 and CD90 and negative for CD45 and CD31, having similar phenotypes to the non-treated MSC.

groups compared with the control group ( $P < 0.01$ ; Figure 2C).

Placement of MSC adjacent to PC3 cells induced characteristic re-organization of actin filaments, as detected by immunofluorescence, which was not observed in BMSC cultured in the control agarose pellet-only group, and the F-actin filaments were randomly organized (Figure 2D). In the presence of the PC3 tumor cell pellet, most of the actin filaments were parallel-oriented toward

tumor cells, and BMSC were an elongated rod shape (Figure 2E).

#### *Expression of chemokine, cytokine receptors and MMP in BMSC with tumor CM stimulation*

Nineteen chemokine/cytokine receptors and MMP [CCR1, CCR2, CCR3, CCR4, CCR5, CCR6, CCR7, CCR9, CX3CR1, CXCR3, CXCR4, Human growth

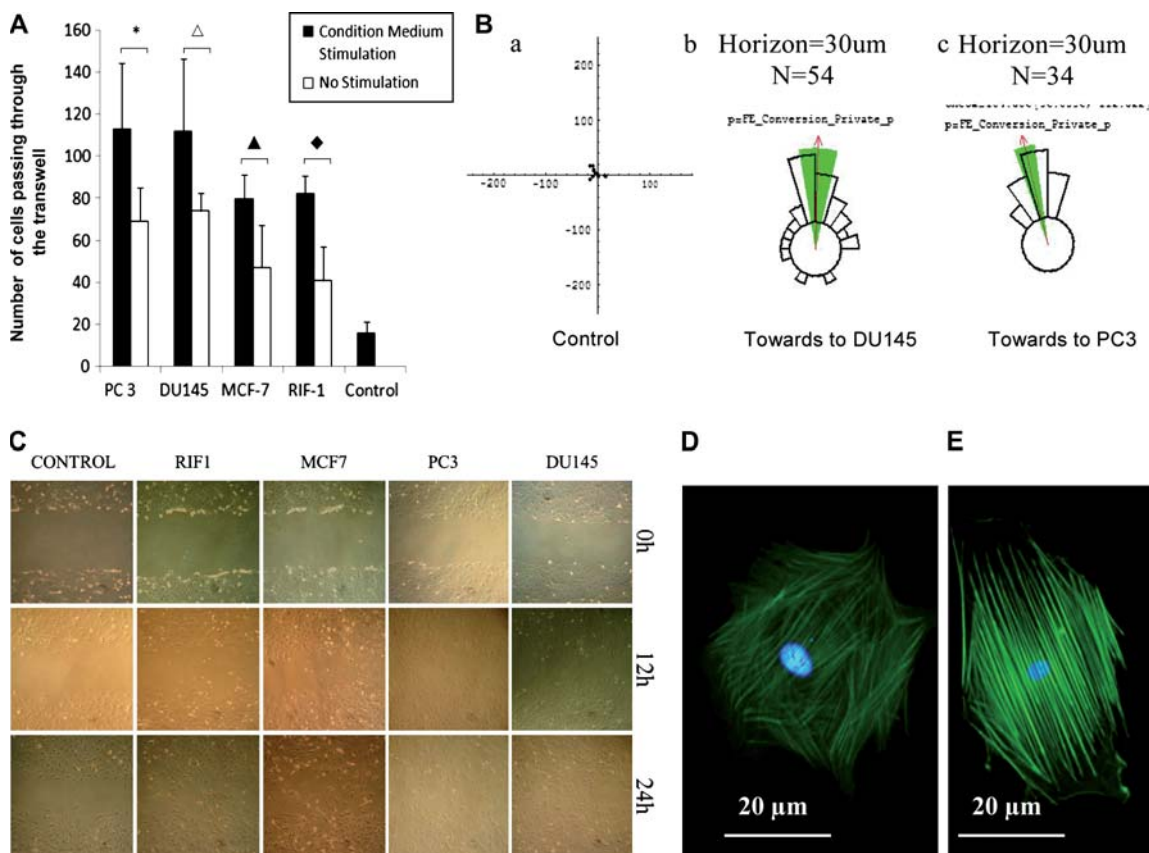


Figure 2. (A) Transwell migration of BMSC toward tumor cells with or without tumor CM pre-treatment. The dark bars represent migration to tumor cells after CM treatment while the lighter bars represent migration without CM treatment for the BMSC. Significantly more BMSC migrated through the membranes when the BMSC were pre-treated with CM of tumors cells compared with cells without CM pre-treatment ( $P < 0.01$ ). Data are presented as mean  $\pm$  SD, \* $t = 2.803$ ,  $\Delta t = 2.419$ ,  $\blacktriangle t = 3.126$ ,  $\blacklozenge t = 5.078$ ,  $P < 0.01$ . (B) The Dunn chemotaxis assay results. Circular histograms show the proportion of cells with a direction of migration lying within a given  $20^\circ$  interval. The arrows and the black segment represent the mean significant direction of migration with a 99% confidence interval ( $P < 0.01$ , Rayleigh test, with (a) normal culture medium in the outer ring showing random cell movements and (b)  $1 \times 10^6$  DU145 cells in the outer ring and (c)  $1 \times 10^6$  PC3 cells in the outer ring all showing BMSC movement toward tumor cells. 'N' denotes the total cell numbers tracked each time and a minimum of 30 was required for statistical analysis. 'Horizon' represents the distance from the starting point to a virtual horizon, which was chosen to be 30  $\mu\text{m}$  for all the experiments and only cells migrating to this distance or beyond were used for data analysis. (C) Wound and healing assay showed that the scratching gap distances were significantly reduced at 12 and 24 h in the groups treated with tumor CM in the various tumor cell lines tested. (D) PC3 tumor cell-agarose pellet and BMSC co-culture system for the actin polymerization assay. The actin filaments in the BMSC-only culture were randomly arranged. (E) Exposure of MSC to PC3 tumor cells altered F-actin filament organization; all F-actin filaments were arranged perpendicular to the tumor cells, indicating their migration toward tumor cells. Bar = 20  $\mu\text{m}$ .

hormone-releasing factor (HGRF), Beta-type platelet-derived growth factor receptor PDGFR $\beta$ , EGF receptor; epidermal growth factor receptor (EGFR), MMP-2, MMP-9, MMP-14, Tissue inhibitor of metalloproteinases TIMP-1 and TIMP-2] and housekeeping genes were tested by PCR. CCR3, CXCR4, EGFR, MMP-2, TIMP-1 and TIMP-2 were normally expressed in the BMSC (control lane, Figure 3A). After 24 h of various tumor CM stimulation, expression of CXCR4 was upregulated; EGFR expression was downregulated and TIMP-1, TIMP-2, MMP-2 expression did not differ significantly (Figure 3A). MMP-2 mRNA expression was seen in normal BMSC and remained unchanged during 24-h tumor CM treatments. However, Western blot data showed

that MMP-2 protein was not expressed in the BMSC, but after 2-h exposure to the tumor CM, MMP-2 protein expression was upregulated in the BMSC in all the groups and downregulated at 24 h (Figure 3B). The upregulation of CXCR4 in BMSC after tumor CM stimulation was also confirmed by Western blot (Figure 3B).

#### Homing of BMSC to tumor sites *in vitro* and *in vivo*

The migration of BMSC toward tumor cells was inhibited significantly by the MMP-2 inhibitor in all the tumor cells tested, while the CXCR4 inhibitor AMD3100 inhibited BMSC migration toward PC3, MCF-7 and RIF-1 cells ( $P < 0.001$ ) but not

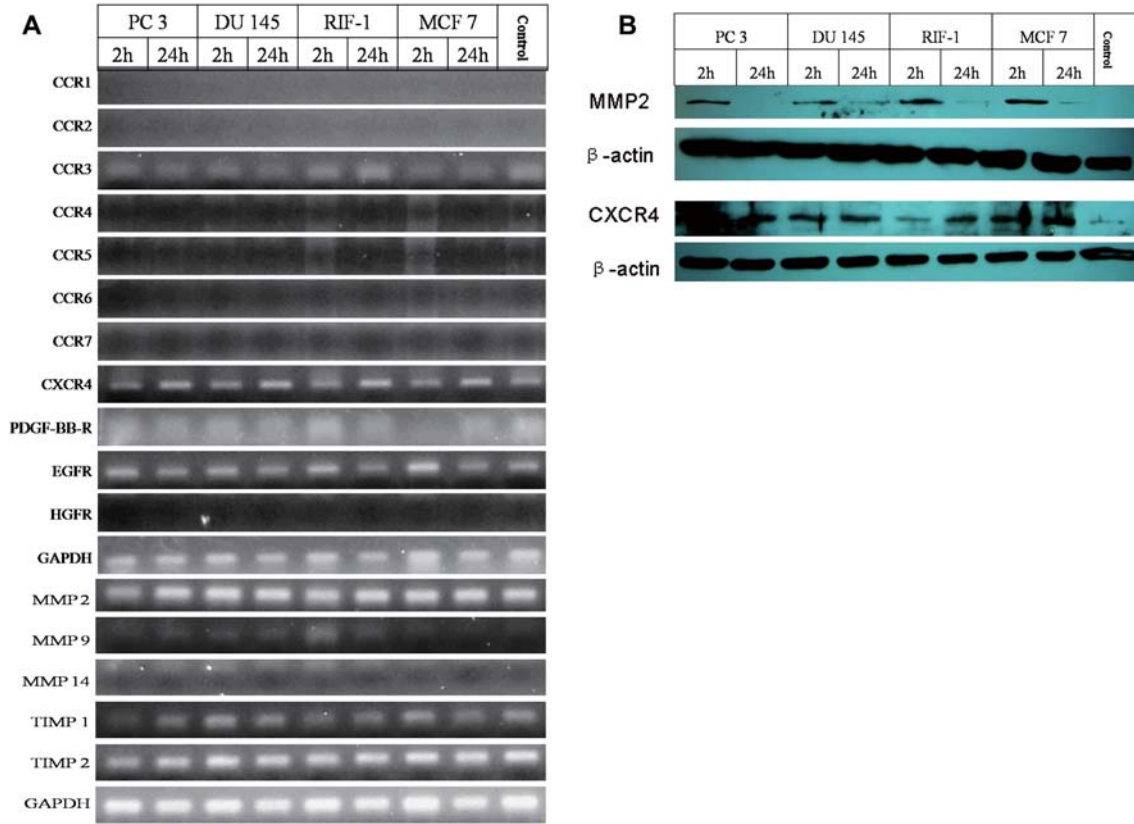


Figure 3. (A) Expression of MMP and their inhibitors, and chemokine and cytokine receptors, before and after tumor CM stimulation. CCR3, CXCR4, EGFR, MMP-2, TIMP-1 and TIMP-2 were normally expressed in BMSC. After 24 h of tumor CM exposure, PCR results showed that CXCR4 was upregulated and EGFR was downregulated. (B) The changes in CXCR4 and MMP-2 expression in BMSC at the protein level were also checked by Western blot. MMP-2 was not detected in normal BMSC; after 2 h exposure to tumor CM, MMP-2 protein was expressed in the BMSC and it was downregulated after 24 h exposure to tumor CM.

DU145 cells (Figure 4). In the subcutaneous tumor implantation model, BMSC were mainly engrafted at the tumor sites as early as 3 days after i.v. injection and the engrafted BMSC survived and expressed the luciferase gene for up to 12 days in the tumor sites (Figure 5A). Some of the BMSC also migrated into the lung and spleen at the early time-points and there were redistributions of BMSC in the DU145 tumor model, where more BMSC migrated to the lung in the later time-points at 9 and 12 days following their injection (Figure 5B). The distributions of systemically administrated BMSC in various organs of the mice were examined at the termination point, as shown in Figure 5C. Some BMSC engrafted in lung, spleen and liver, and none in brain and kidney; the majority of BMSC were seen in the tumors. BMSC were further identified with anti-EGFP antibody in the tumor stroma and parenchyma in both PC3 and DU145 tumor masses at day 12 following MSC administration (Figure 5D).

In the lung metastatic model of PC3 tumor cells, after i.v. infusion of a single dose of BMSC, the distribution of BMSC was monitored by *in vivo* imaging over a period of 30 days. The change in distribution of

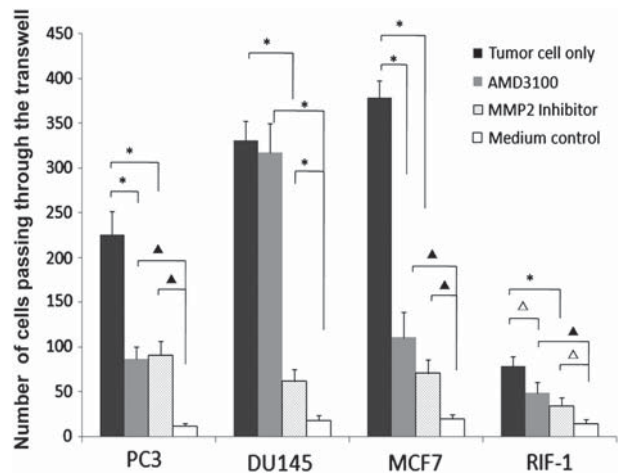


Figure 4. Addition of the inhibitor to CXCR4 or MMP-2 in the culture system resulted in partial inhibition of BMSC migration toward the tumor cells. In PC3, MCF-7 and RIF-1 cells, both CXCR4 inhibitor (AMD3100) and MMP-2 inhibitor significantly inhibited the BMSC migration ( $P < 0.001$ ). In DU145 cells, only the MMP-2 inhibitor showed an inhibitory effect on BMSC migration. The numbers of BMSC migrating toward all tumor cells even in the presence of CXCR4 or MMP-2 inhibitors were significantly higher than those in the control group where no tumor cells were present ( $*P < 0.001$ ,  $\Delta P < 0.005$ ,  $\blacktriangle P < 0.01$ ). Data are presented as mean  $\pm$  SD.

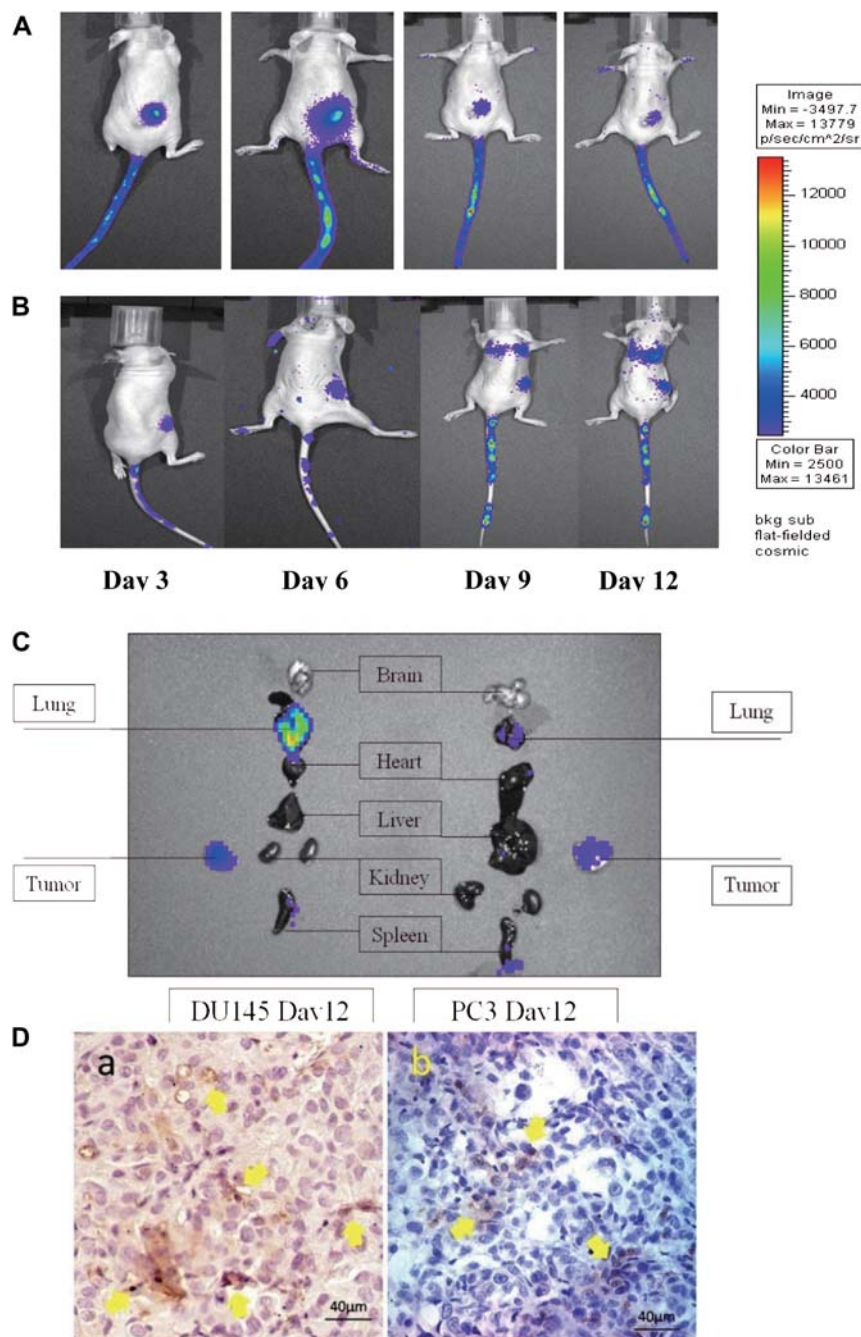


Figure 5. (A) Distribution of Luc-BMSC in PC3 (A) and DU145 (B) subcutaneous tumor models. BMSC engrafted into the tumor sites as early as 3 days. The BMSC survived and expressed the luciferase gene for up to 12 days in the tumors. (B) Redistribution of Luc-BMSC from the tumor sites to lung and other organs was observed in mice bearing DU145 tumor cells at days 9 and 12. (C) In the subcutaneous tumor model, the tumor-bearing animals were terminated at 4 weeks following tumor implantation (2 weeks after Luc-BMSC systemic injection) and their internal organs were removed and subjected to *in vivo* imaging examinations. It was shown that a few Luc-BMSC were still engrafted in the lung and liver but the majority of the Luc-BMSC were seen in the tumors. (D) The engraftment of BMSC in the tumor parenchyma in the PC3 lung metastasis model was confirmed by immunostaining of GFP-positive cells (arrows; a, PC3 tumor tissues; b, DU145 tumor tissues).

BMSC over time is shown in Figure 6A. The majority of BMSC engrafted in the lung at day 1 of injection and some of them were retained in the lung till 30 days. The percentage of bioluminescent signals in the lung compared with the whole body was quantified using the *in vivo* imaging software and is shown in

Figure 5B. At day 1 after BMSC infusion,  $95.02 \pm 4.80\%$  BMSC were in the lung; the number reduced to  $39.39 \pm 14.86\%$  at day 3,  $26.63 \pm 5.05\%$  at day 14 and  $36 \pm 1.37\%$  at day 30 (Figure 6B). The presence of BMSC in the lung tumor stroma was confirmed by positive staining of EGFP antibody at day 30 (Figure 6C).

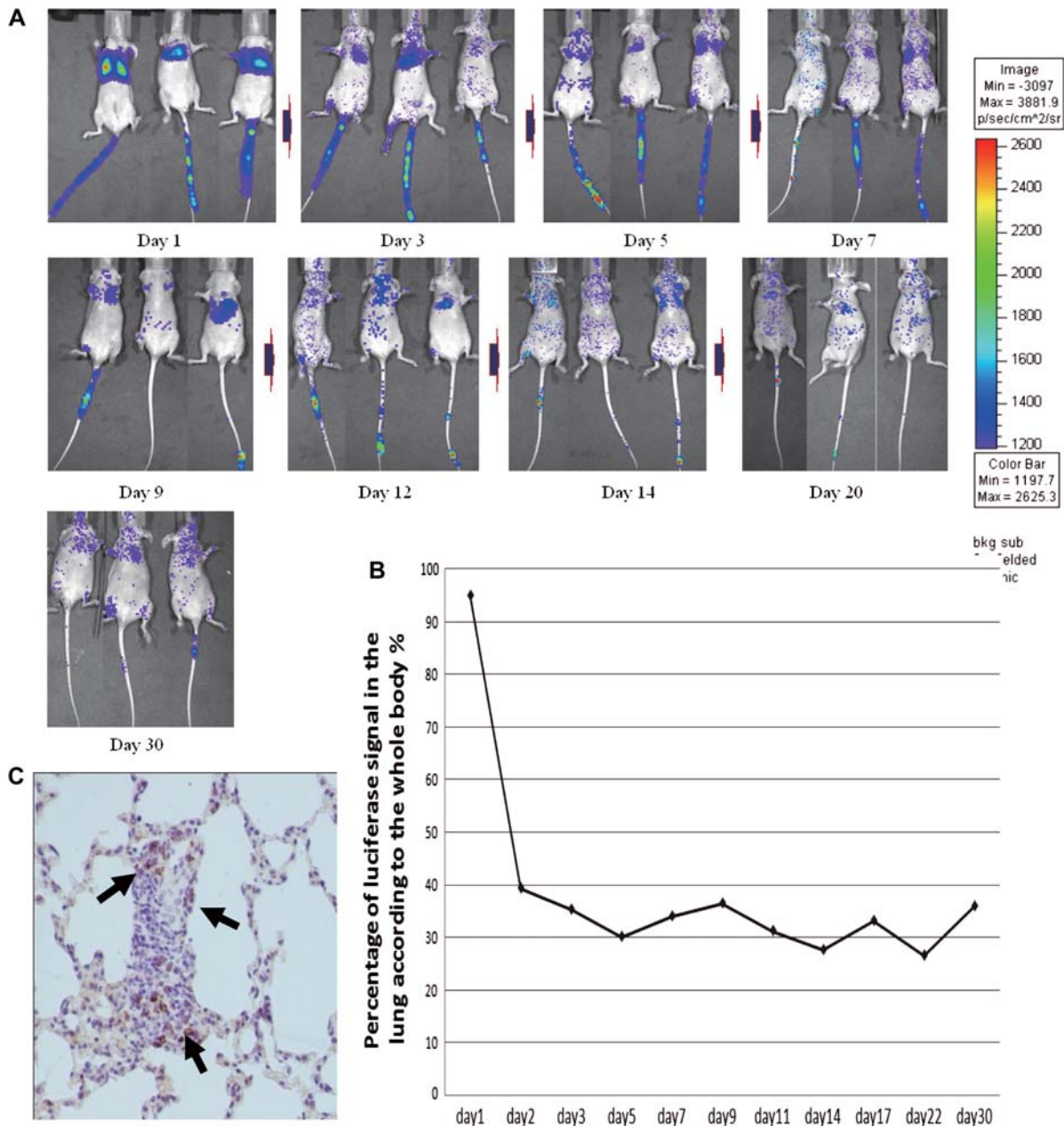


Figure 6. *In vivo* distribution of BMSC in the PC3 cell lung metastasis model. After i.v. infusion of a single dose of Luc-BMSC, bioluminescent images were taken at nine time-points over 30 days. (A) The change of distribution of BMSC over time. (B) Percentage of BMSC in the lung compared with total BMSC in the body. More than 95% of the BMSC were trapped in the lung following injection at day 1, and from day 2 the number of BMSC in the lung dropped to around 40% and the percentage remain unchanged till day 30. (C) The presence of BMSC in the tumor stroma and parenchyma was confirmed by positive immunostaining of EGFP (brown cells, arrows).

## Discussion

BMSC have the ability to migrate to sites of injury, inflammation and tumors. However, the molecular events underlying the specific migration of BMSC are not well defined. Understanding the signaling pathways associated with migration of BMSC will help to define the role of BMSC in tumor growth as well as use them as delivery vehicles for site-specific therapy. The present study investigated the migration ability

of BMSC toward tumor cells *in vitro* and *in vivo*, and the possible cytokines, chemokines and their receptors involved in the process.

We tested the migration of rat BMSC toward four tumor cell lines, two human prostate cancer cell lines (PC3 and DU145), one human breast cancer cell line (MCF-7) and a mouse fibrosarcoma cell line (RIF-1). Among them, PC3, DU145 and MCF-7 are all metastatic human tumor cell lines, and RIF-1 is a radiation-induced fibrosarcoma cell

line from mice. The migration of BMSC toward all four tumor cell lines was demonstrated *in vitro*, consistent with previous reports (6). *In vivo* experiments further confirmed the homing of rat BMSC to PC3 and DU145 tumor sites in both subcutaneous and lung metastatic tumor models. The homing of rat BMSC to the tumor sites occurred rapidly following their i.v. infusion; most of the cells engrafted in the tumor sites within 3 days of injection. Although some of the BMSC were found in organs other than the tumor, their quantity was low compared with the tumor sites. Furthermore, the BMSC survived and expressed functional luciferase gene in the tumor microenvironments for prolonged period, for example 30 days, suggesting that these cells can survive inside the tumors and are ideal vehicles for delivery of anti-tumor agents. As shown by us and others, BMSC were found both in the parenchyma and stroma of the tumors (26–28), so that the therapeutic substances secreted by the BMSC could reach most of the tumor cells to produce maximal effects.

It has been well documented that human MSC can migrate to human tumors in SCID mice (7,28). We have also demonstrated that rat MSC can home to mouse fibrosarcoma developed in the C3H mouse, and genetically modified rat iNOS-MSM had anti-tumor effects in a mouse tumor model (29). We and others have demonstrated that MSC are immunosuppressive cells and they do not trigger acute immunoresponses (22); even xenogenic MSC can survive *in vivo* for prolonged periods (30). Therefore MSC may share similar tumor-homing characteristics regardless of their species.

The reasons we used rat MSC as a study tool are: (a) we have GFP rats readily available and the GFP is stably expressed in all tissues of the rat, including BMSC, making them a good cell source for study because they are easy to harvest and culture, and easy to trace *in vitro* and *in vivo* (with antibody to GFP on paraffin sections); (b) we have pilot experimental results both *in vitro* and *in vivo* demonstrating that rat MSC have similar tumor tropisms as human MSC toward human tumor cells; (c) the *in vivo* tumor animal model is established using immunocompromised (nude) mice, so there was no concern about the specie specificity in this study because there was no immunity issues in the model. Because of these reasons and based on the pilot data, we carried out the present study using rat MSC as a study vehicle. It would have been better if we had used human or mouse MSC to carry out similar experiments, but the results obtained from the current study do serve the purpose of addressing some mechanisms of BMSC homing to tumor cells *in vitro* and *in vivo*. The data also clearly demonstrate that MSC, regardless of species, have similar tumor tropism abilities *in vivo*.

The mechanisms by which rat BMSC home and engraft to human tumors are not yet fully understood or defined; it is likely that tumor tissues express some specific ligands to facilitate trafficking, adhesion and infiltration of rat BMSC (31). Based on the microarray data in the literature (6), we selected and tested 19 chemokines and cytokine receptors in this study, whose ligands were potentially amongst the strongest chemo-attractants for BMSC. We found that CCR3, CXCR4, EGFR, MMP-2, TIMP-1 and TIMP-2 were expressed in normal BMSC; after 24 h of tumor CM exposure, CXCR4 was upregulated but EGFR was downregulated. Western blot showed that MMP-2 was upregulated after 2 h exposure with tumor CM and downregulated after 24 h. The results suggested that the migration of BMSC is a multistep process. The tumor cells and their microenvironments secreted chemokines or cytokines, as demonstrated in the CM studies, which could upregulate the expression of chemokines and cytokine receptors on the BMSC (10,32). Shortly after receiving tumor stimuli, some chemokine receptors such as CXCR4 are upregulated in BMSC, as we and others have demonstrated (14). After tumor CM stimulation, BMSC had enhanced their migration ability toward tumor cells, which could be attributed to the upregulation of CXCR4 on BMSC. The SDF-1 released from the tumor sites may serve as a strong chemoattractant for the BMSC (33). The morphologic changes of BMSC when placed adjacent to the tumor cells were revealed by F-actin polymerization assay, in which we have demonstrated the cytoskeletal re-organization of BMSC, a necessary step for cell migration/movement (34). Some receptors that are known to control cell proliferation, such as EGFR, were downregulated in BMSC after tumor CM treatment, and this may prepare the cells to migrate. The upregulation of MMP-2 at an early stage of CM stimulation may be a necessary step to prepare the BMSC for detaching and invading into the extracellular matrices of tumors, which is also observed in the migration of BMSC and other stem cells across vascular basement membranes (35,36).

Our data suggest that both CXCR4 and MMP-2 may be involved in the migration of BMSC toward tumors. However, AMD3100 (the specific inhibitor of CXCR4) and an MMP-2 inhibitor could not totally abolish the migration of BMSC toward tumor cells, suggesting that there must be other factors involved in the specific migration of BMSC to tumors. Interestingly, the CXCR4 inhibitor did not affect the migration of BMSC toward DU145 cells, indicating that different tumors may employ different mechanisms in attracting BMSC. Other molecules, such as integrin, also play a role in different stages of the BMSC homing process (37,38). It is unclear whether

several factors operate synergistically in response to distinct stimuli such as trauma, inflammation and tumor. It is, therefore, important to determine the roles of chemokine/cytokine factors in different types of tumors and their relation to BMSC tumor homing. To elucidate further the mobilization mechanisms of BMSC, detection of cytokines released from the tumor sites, analysis of receptors on BMSC and the downstream signal transduction pathways following interaction between these receptors and ligands should be the focus of future studies.

The *in vitro* migration assay represents only a small part of the process of MSC homing to tumors. The *in vivo* homing of BMSC is more complex. The tumor cells could secrete many cytokines and chemokines to regulate BMSC homing, as well as the hypoxic conditions inside the tumor. There are also barriers for BMSC to pass through during their homing process, such as the bone marrow endothelium, subendothelial basement membranes (36), lung barrier (39) and blood–cerebral barrier (40). A key requirement for cells to reach the distant target sites is the ability to traverse the ECM that is present between cells of all tissue types. Basement membranes represent a specialized form of the ECM that separates epithelium or endothelium from stroma by a dense layer of ECM. To overcome these matrix barriers, migrating cells require specific proteolytic enzymes (14,21,31). Our data show that MMP-2 protein was not expressed in normal BMSC, upregulated after 2 h of tumor CM treatment and downregulated at 24 h, suggesting that MMP-2 expression is tightly regulated, probably through tissue inhibitor of matrix metalloproteinase (TIMP)-1 and TIMP-2 at different stages of BMSC homing/engrafting into tumors. Taken together, these data suggest that MMP-2, which has the capacity to degrade a major constituent basement membrane, collagen IV, and CXCR4 might play important roles in mediating BMSC migration toward tumors *in vivo*.

In conclusion, we have shown that rat BMSC are able to migrate toward four different human and mouse tumor cells *in vitro*, and home to both subcutaneous and lung metastatic prostate tumor models *in vivo*, suggesting that xenogenic BMSC are capable of specifically homing into tumor tissues, similar to autologous MSC. Analysis of the gene expression revealed that MMP-2 transcripts were upregulated after short-term exposure to tumor CM but downregulated after longer term exposure. CXCR4 upregulation was also found in BMSC after 24 h exposure to tumor. Exposure to tumor CM *in vitro* enhanced migration of BMSC toward the tumors *in vivo*. SDF-1

inhibitor AMD3100 and MMP-2 inhibitor partly abolished the BMSC migration toward tumor cells *in vitro*. These results suggest that the CXCR4 and MMP-2 are likely candidates in the multi-step processes of BMSC homing to tumors, and modification of their expression may lead to novel anti-tumor therapies.

### Acknowledgement

We acknowledge the financial support of China Natural Science Foundation (grant number 30872635/C160705) to GL, Hong Kong Innovation Technology Commission (grant reference ITS/09/305) to GL and a Direct Research Grant from The Medical Faculty, The Chinese University of Hong Kong (2041522) to GL.

**Declaration of interest:** The authors report no conflicts of interest. The authors alone are responsible for the content and writing of the paper.

### References

1. Sasaki M, Abe R, Fujita Y, Ando S, Inokuma D, Shimizu H. Mesenchymal stem cells are recruited into wounded skin and contribute to wound repair by transdifferentiation into multiple skin cell type. *J Immunol.* 2008;180(4):2581–7.
2. Fukuda K, Fujita J. Mesenchymal, but not hematopoietic, stem cells can be mobilized and differentiate into cardiomyocytes after myocardial infarction in mice. *Kidney Int.* 2005;68(5):1940–3.
3. Klopp AH, Spaeth EL, Dembinski JL, Woodward WA, Munshi A, Meyn RE, et al. Tumor irradiation increases the recruitment of circulating mesenchymal stem cells into the tumor microenvironment. *Cancer Res.* 2007;67(24):11687–95.
4. Kashofer K, Bonnet D. Gene therapy progress and prospects: stem cell plasticity. *Gene Ther.* 2005;12(16):1229–34.
5. Dvorak HF. Tumors: wounds that do not heal. Similarities between tumor stroma generation and wound healing. *N Engl J Med.* 1986;315(26):1650–9.
6. Menon LG, Picinich S, Koneru R, Gao H, Lin SY, Koneru M, et al. Differential gene expression associated with migration of mesenchymal stem cells to conditioned medium from tumor cells or bone marrow cells. *Stem Cells* 2007;25(2):520–8.
7. Dwyer RM, Potter-Beirne SM, Harrington KA, Lowery AJ, Hennessy E, Murphy JM, et al. Monocyte chemotactic protein-1 secreted by primary breast tumors stimulates migration of mesenchymal stem cells. *Clin Cancer Res.* 2007;13(17):5020–7.
8. Sordi V, Malosio ML, Marchesi F, Mercalli A, Melzi R, Giordano T, et al. Bone marrow mesenchymal stem cells express a restricted set of functionally active chemokine receptors capable of promoting migration to pancreatic islets. *Blood.* 2005;106(2):419–27.
9. Ringe J, Strassburg S, Neumann K, Endres M, Nötter M, Burmester GR, et al. Towards in situ tissue repair: human mesenchymal stem cells express chemokine receptors CXCR1, CXCR2 and CCR2, and migrate upon stimulation with CXCL8 but not CCL2. *J Cell Biochem.* 2007;101(1):135–46.

10. Croitoru-Lamoury J, Lamoury FM, Zaunders JJ, Veas LA, Brew BJ. Human mesenchymal stem cells constitutively express chemokines and chemokine receptors that can be upregulated by cytokines, IFN-beta, and Copaxone. *J Interferon Cytokine Res.* 2007;27(1):53–64.
11. Ponte AL, Marais E, Gallay N, Langonné A, Delorme B, Héroult O, et al. The in vitro migration capacity of human bone marrow mesenchymal stem cells: comparison of chemokine and growth factor chemotactic activities. *Stem Cells.* 2007;25(7):1737–45.
12. Honczarenko M, Le Y, Swierkowski M, Ghiran I, Glodek AM, Silberstein LE. Human bone marrow stromal cells express a distinct set of biologically functional chemokine receptors. *Stem Cells.* 2006;24(4):1030–41.
13. Tomchuck SL, Zvezdaryk KJ, Coffelt SB, Waterman RS, Danka ES, Scandurro AB. Toll-like receptors on human mesenchymal stem cells drive their migration and immunomodulating responses. *Stem Cells.* 2008;26(1):99–107.
14. Son BR, Marquez-Curtis LA, Kucia M, Wysoczynski M, Turner AR, Ratajczak J, et al. Migration of bone marrow and cord blood mesenchymal stem cells in vitro is regulated by stromal-derived factor-1-CXCR4 and hepatocyte growth factor-c-met axes and involves matrix metalloproteinases. *Stem Cells.* 2006;24(5):1254–64.
15. Guo J, Lin G, Bao C, Hu Z, Chu H, Hu M. Insulin-like growth factor 1 improves the efficacy of mesenchymal stem cells transplantation in a rat model of myocardial infarction. *J Biomed Sci.* 2008;15(1):89–97.
16. Li Y, Yu X, Lin S, Li X, Zhang S, Song YH. Insulin-like growth factor 1 enhances the migratory capacity of mesenchymal stem cells. *Biochem Biophys Res Commun.* 2007;356(3):780–4.
17. Fiedler J, Brill C, Blum WF, Brenner RE. IGF-I and IGF-II stimulate directed cell migration of bone-marrow-derived human mesenchymal progenitor cells. *Biochem Biophys Res Commun.* 2006;345(3):1177–83.
18. Schichor C, Birnbaum T, Etmann N, Schnell O, Grau S, Miebach S, et al. Vascular endothelial growth factor A contributes to glioma-induced migration of human marrow stromal cells (hMSC). *Exp Neurol.* 2006;199(2):301–10.
19. Ozaki Y, Nishimura M, Sekiya K, Suehiro F, Kanawa M, Nikawa H, et al. Comprehensive analysis of chemotactic factors for bone marrow mesenchymal stem cells. *Stem Cells Dev.* 2007;16(1):119–29.
20. Burger JA, Kipps TJ. CXCR4: a key receptor in the crosstalk between tumor cells and their microenvironment. *Blood.* 2006;107(5):1761–7.
21. Ries C, Egea V, Karow M, Kolb H, Jochum M, Neth P. MMP-2, MT1-MMP, and TIMP-2 are essential for the invasive capacity of human mesenchymal stem cells: differential regulation by inflammatory cytokines. *Blood.* 2007;109(9):4055–63.
22. Chen X, McClurg A, Zhou GQ, McCaigue M, Armstrong MA, Li G. Chondrogenic differentiation alters the immunosuppressive property of bone marrow-derived mesenchymal stem cells, and the effect is partially due to the upregulated expression of B7 molecules. *Stem Cells.* 2007;25(2):364–70.
23. Wells CM, Ridley AJ. Analysis of cell migration using the Dunn chemotaxis chamber and time-lapse microscopy. *Methods Mol Biol.* 2005;294:31–41.
24. Guan JL. Cell Migration: Developmental Methods and Protocols. *Methods in Molecular Biology.* 2003;294:23–29.
25. Meriane M, Duhamel S, Lejeune L, Galipeau J, Annabi B. Cooperation of matrix metalloproteinases with the RhoA/Rho kinase and mitogen-activated protein kinase kinase-1/extracellular signal-regulated kinase signaling pathways is required for the sphingosine-1-phosphate-induced mobilization of marrow-derived stromal cells. *Stem Cells.* 2006;24(11):2557–65.
26. Nakamura K, Ito Y, Kawano Y, Kurozumi K, Kobune M, Tsuda H, et al. Antitumor effect of genetically engineered mesenchymal stem cells in a rat glioma model. *Gene Ther.* 2004;11(14):1155–64.
27. Kucerova L, Altanerova V, Matuskova M, Tyciakova S, Altaner C. Adipose tissue-derived human mesenchymal stem cells mediated prodrug cancer gene therapy. *Cancer Res.* 2007;67(13):6304–13.
28. Studeny M, Marini FC, Dembinski JL, Zompetta C, Cabreira-Hansen M, Bekele BN, et al. Mesenchymal stem cells: potential precursors for tumor stroma and targeted-delivery vehicles for anticancer agents. *J Natl Cancer Inst.* 2004;96(21):1593–603.
29. Xiang J, Tang JQ, Song C, Yang Z, Hirst DG, Zheng QJ, et al. Mesenchymal stem cells as a gene therapy carrier for treatment of fibrosarcoma. *Cytotherapy.* 2009;26:1–11.
30. Wang Y, Chen X, Armstrong M, Li G. Survival of xenogeneic bone marrow-derived mesenchymal stem cells in a xenotransplantation model. *J Orthop Res.* 2007;25:926–932.
31. Spaeth E, Klopp A, Dembinski J, Andreeff M, Marini F. Inflammation and tumor microenvironments: defining the migratory itinerary of mesenchymal stem cells. *Gene Ther.* 2008;15(10):730–8.
32. Shi M, Li J, Liao L, Chen B, Li B, Chen L, et al. Regulation of CXCR4 expression in human mesenchymal stem cells by cytokine treatment: role in homing efficiency in NOD/SCID mice. *Haematologica.* 2007;92(7):897–904.
33. Orimo A, Gupta PB, Sgroi DC, Arenzana-Seisdedos F, Delaunay T, Naeem R, et al. Stromal fibroblasts present in invasive human breast carcinomas promote tumor growth and angiogenesis through elevated SDF-1/CXCL12 secretion. *Cell.* 2005;121(3):335–48.
34. Lauffenburger DA, Horwitz AF. Cell migration: a physically integrated molecular process. *Cell.* 1996;84(3):359–69.
35. Mannello F. Multipotent mesenchymal stromal cell recruitment, migration, and differentiation: what have matrix metalloproteinases got to do with it? *Stem Cells.* 2006;24(8):1904–7.
36. De Becker A, Van Hummelen P, Bakkus M, Vande Broek I, De Wever J, De Waele M, et al. Migration of culture-expanded human mesenchymal stem cells through bone marrow endothelium is regulated by matrix metalloproteinase-2 and tissue inhibitor of metalloproteinase-3. *Haematologica.* 2007;92(4):440–9.
37. Ip JE, Wu Y, Huang J, Zhang L, Pratt RE, Dzau VJ. Mesenchymal stem cells use integrin beta1 not CXC chemokine receptor 4 for myocardial migration and engraftment. *Mol Biol Cell.* 2007;18(8):2873–82.
38. Schmidt A, Ladage D, Schinkothe T, Klausmann U, Ulrichs C, Klinz FJ, et al. Basic fibroblast growth factor controls migration in human mesenchymal stem cells. *Stem Cells.* 2006;24(7):1750–8.
39. Schrepfer S, Deuse T, Reichenspurner H, Fischbein MP, Robbins RC, Pelletier MP. Stem cell transplantation: the lung barrier. *Transplant Proc.* 2007;39(2):573–6.
40. Kim JM, Lee ST, Chu K, Jung KH, Song EC, Kim SJ, et al. Systemic transplantation of human adipose stem cells attenuated cerebral inflammation and degeneration in a hemorrhagic stroke model. *Brain Res.* 2007;1183:43–50.